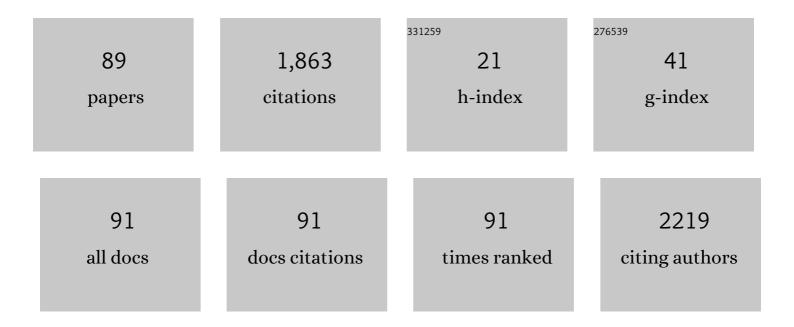
## Francesco Conversano

List of Publications by Year in descending order

Source: https://exaly.com/author-pdf/6959055/publications.pdf Version: 2024-02-01



#	Article	IF	CITATIONS
1	Automatic measurement of head-perineum distance during intrapartum ultrasound: description of the technique and preliminary results. Journal of Maternal-Fetal and Neonatal Medicine, 2022, 35, 2759-2764.	0.7	3
2	Novel artificial intelligence approach for automatic differentiation of fetal occiput anterior and nonâ€occiput anterior positions during labor. Ultrasound in Obstetrics and Gynecology, 2022, 59, 93-99.	0.9	9
3	Pulse-Echo Measurements of Bone Tissues. Techniques and Clinical Results at the Spine and Femur. Advances in Experimental Medicine and Biology, 2022, 1364, 145-162.	0.8	1
4	New technique for automatic sonographic measurement of change in head–perineum distance and angle of progression during active phase of second stage of labor. Ultrasound in Obstetrics and Gynecology, 2020, 56, 597-602.	0.9	8
5	Radiofrequency echographic multispectrometry compared with dual X-ray absorptiometry for osteoporosis diagnosis on lumbar spine and femoral neck. Osteoporosis International, 2019, 30, 391-402.	1.3	56
6	Ultrasound Fragility Score: An innovative approach for the assessment of bone fragility. Measurement: Journal of the International Measurement Confederation, 2017, 101, 236-242.	2.5	21
7	Automatic ultrasound technique to measure angle of progression during labor. Ultrasound in Obstetrics and Gynecology, 2017, 50, 766-775.	0.9	12
8	Human Hepatocarcinoma Cell Targeting by Glypican-3 Ligand Peptide Functionalized Silica Nanoparticles: Implications for Ultrasound Molecular Imaging. Langmuir, 2017, 33, 4490-4499.	1.6	15
9	Simulated Measurements of the Magnetic Behavior of New Dual-Mode Nanosized Contrast Agents. IEEE Nanotechnology Magazine, 2017, 16, 842-850.	1.1	2
10	A quantitative ultrasound approach to estimate bone fragility: A first comparison with dual X-ray absorptiometry. Measurement: Journal of the International Measurement Confederation, 2017, 101, 243-249.	2.5	23
11	MODELING AND DESIGNING A FULL BEAMFORMER FOR ACOUSTIC SENSING AND MEASUREMENT. International Journal on Smart Sensing and Intelligent Systems, 2017, 10, 718-734.	0.4	3
12	Automatic Echographic Detection of Halloysite Clay Nanotubes in a Low Concentration Range. Nanomaterials, 2016, 6, 66.	1.9	6
13	Major osteoporotic fragility fractures: Risk factor updates and societal impact. World Journal of Orthopedics, 2016, 7, 171.	0.8	344
14	Determining Shapes and Sizes Using TEM Images: Functionalized Nanoparticles. , 2016, , .		1
15	An Advanced Quantitative Echosound Methodology for Femoral Neck Densitometry. Ultrasound in Medicine and Biology, 2016, 42, 1337-1356.	0.7	33
16	Surface Coating Highly Improves Cytocompatibility of Halloysite Nanotubes: A Metabolic and Ultrastructural Study. IEEE Nanotechnology Magazine, 2016, 15, 770-774.	1.1	16
17	A new approach for measuring the trabecular bone density through the echosound backscattering: An ex vivo validation on human femoral heads. Measurement: Journal of the International Measurement Confederation, 2016, 87, 51-61.	2.5	10
18	Inâ€vitro study of human proximal femur microstructure: analysis of the relationship between microâ€computed tomography data and quantitative ultrasound parameters. IET Science, Measurement and Technology, 2016, 10, 193-199.	0.9	6

#	Article	IF	CITATIONS
19	Automatic method for vertebral morphometry measurements. IET Science, Measurement and Technology, 2016, 10, 327-334.	0.9	2
20	Innovative ultrasound approach to estimate spinal mineral density: diagnostic assessment on overweight and obese women. IET Science, Measurement and Technology, 2016, 10, 1-9.	0.9	5
21	Estimation of femoral neck bone mineral density by ultrasound scanning: Preliminary results and feasibility. Measurement: Journal of the International Measurement Confederation, 2016, 94, 480-486.	2.5	11
22	EEG signal processing and acquisition for detecting abnormalities via bio-implantable devices. , 2016, , .		9
23	Model simulations and comparative evaluations of susceptibility-based and gadolinium contrast enhancement for high-resolution brain venography. , 2016, , .		Ο
24	Validation of an automatic segmentation method to detect vertebral interfaces in ultrasound images. IET Science, Measurement and Technology, 2016, 10, 18-27.	0.9	6
25	Measuring Lung Abnormalities In Images-Based Ct. International Journal on Smart Sensing and Intelligent Systems, 2016, 9, 1156-1176.	0.4	10
26	Effective Targeting of Hepatocellular Carcinoma through Glypican-3 Ligand Peptide Functionalization of Silica Nanoparticles. , 2015, , .		1
27	A Dual Frequency Ultrasound Technique for the Improved Detection of Bimodal Nanosized Contrast Agents. , 2015, , .		0
28	Comparative Assessment of the MRI Enhancement Power of Novel Nanosystems Through Theoretical Simulations. , 2015, , .		0
29	Highly Improved Cytocompatibility of Halloysite Nanotubes through Polymeric Surface Modification. , 2015, , .		1
30	Nanocircuits for a Bio-Implantable System in EEG Signal Acquisitions. , 2015, , .		1
31	Ultrasound Signal Enhancement of Halloysite Clay Nanotubes at Medical Diagnostic Frequencies. , 2015, , .		1
32	Microsensors and energy harvesting for thermotherapy: Design and characterization. , 2015, , .		1
33	An Innovative Ultrasound Signal Processing Technique to Selectively Detect Nanosized Contrast Agents in Echographic Images. IEEE Transactions on Instrumentation and Measurement, 2015, 64, 2136-2145.	2.4	11
34	Ultrasound Osteoporosis Score: A novel parameter for the estimation of spine mineral density. , 2015, ,		0
35	A new ultrasound parameter for osteoporosis diagnosis: Clinical validation on normal- and under-weight women. , 2015, , .		1
36	Ex-vivo measurements of quantitative ultrasound and micro-CT parameters on intact human femoral heads. , 2015, , .		0

3

#	Article	IF	CITATIONS
37	A Novel Ultrasound Methodology for Estimating Spine Mineral Density. Ultrasound in Medicine and Biology, 2015, 41, 281-300.	0.7	79
38	New perspectives in echographic diagnosis of osteoporosis on hip and spine. Clinical Cases in Mineral and Bone Metabolism, 2015, 12, 142-50.	1.0	17
39	SAT0491â€Accuracy of A New Ultrasonic Method for Osteoporosis Diagnosis on Lumbar Spine. Annals of the Rheumatic Diseases, 2014, 73, 770.3-771.	0.5	0
40	Automatic image detection of Halloysite clay Nanotubes as a future ultrasound theranostic agent for tumoral cell targeting and treatment. , 2014, , .		4
41	Multiparametric Evaluation of the Acoustic Behavior of Halloysite Nanotubes for Medical Echographic Image Enhancement. IEEE Transactions on Instrumentation and Measurement, 2014, 63, 1423-1430.	2.4	20
42	Entropy Index in Quantitative EEG Measurement for Diagnosis Accuracy. IEEE Transactions on Instrumentation and Measurement, 2014, 63, 1440-1450.	2.4	70
43	Laser fluence and exposure time effects on optoacoustic signal from gold nanorods for enhanced medical imaging. , 2014, , .		1
44	Multi-frequency differential image enhancement of nanosized ultrasound contrast agents. , 2014, , .		2
45	Fully automatic 3D segmentation measurements of human liver vessels from contrast-enhanced CT. , 2014, , .		3
46	Cytotoxicity measurements of Halloysite Nanotubes for nanomedicine applications. , 2014, , .		9
47	Thermal image processing for accurate realtime decision making in surgery. , 2014, , .		7
48	SAT0468â€An Innovative Ultrasound-Based Method for the Estimation of Osteoporotic Fracture Risk. Annals of the Rheumatic Diseases, 2014, 73, 763.1-763.	0.5	0
49	Echographic imaging of tumoral cells through novel nanosystems for image diagnosis. World Journal of Radiology, 2014, 6, 459.	0.5	13
50	Epithelial cell biocompatibility of silica nanospheres for contrast-enhanced ultrasound molecular imaging. Journal of Nanoparticle Research, 2013, 15, 1.	0.8	21
51	Assessment of the enhancement potential of Halloysite Nanotubes for echographic imaging. , 2013, , .		11
52	Effectiveness of Functionalized Nanosystems for Multimodal Molecular Sensing and Imaging in Medicine. IEEE Sensors Journal, 2013, 13, 2305-2312.	2.4	16
53	Multispectrum Approach in Quantitative EEG: Accuracy and Physical Effort. IEEE Sensors Journal, 2013, 13, 3331-3340.	2.4	14
54	Iron Oxide-Gold Core-Shell Nanoparticles as Multimodal Imaging Contrast Agent. IEEE Sensors Journal, 2013, 13, 2341-2347.	2.4	15

#	Article	IF	CITATIONS
55	Low-frequency detection in ECG signals and joint EEG-Ergospirometric measurements for precautionary diagnosis. Measurement: Journal of the International Measurement Confederation, 2013, 46, 97-107.	2.5	37
56	A new ultrasonic method for lumbar spine densitometry. , 2013, , .		2
57	Mutidimensional analysis of EEG features using advanced spectral estimates for diagnosis accuracy. , 2013, , .		32
58	Screening and early diagnosis of osteoporosis through X-ray and ultrasound based techniques. World Journal of Radiology, 2013, 5, 398.	0.5	128
59	Automatic Evaluation of Progression Angle and Fetal Head Station through Intrapartum Echographic Monitoring. Computational and Mathematical Methods in Medicine, 2013, 2013, 1-8.	0.7	8
60	Sonographic markers for early diagnosis of fetal malformations. World Journal of Radiology, 2013, 5, 356.	0.5	25
61	Magnetically-coated silica nanospheres for dual-mode imaging at low ultrasound frequency. World Journal of Radiology, 2013, 5, 411.	0.5	14
62	Gold nanorod coating influence on effectiveness and safety in photoacoustic applications. , 2012, , .		0
63	Quantitative and automatic echographic monitoring of labor progression. , 2012, , .		1
64	Advanced spectral analyses for real-time automatic echographic tissue-typing of simulated tumor masses at different compression stages. IEEE Transactions on Ultrasonics, Ferroelectrics, and Frequency Control, 2012, 59, 2692-701.	1.7	16
65	In Vitro Evaluation and Theoretical Modeling of the Dissolution Behavior of a Microbubble Contrast Agent for Ultrasound Imaging. IEEE Sensors Journal, 2012, 12, 496-503.	2.4	35
66	Fully Automatic Segmentations of Liver and Hepatic Tumors From 3-D Computed Tomography Abdominal Images: Comparative Evaluation of Two Automatic Methods. IEEE Sensors Journal, 2012, 12, 464-473.	2.4	47
67	Echographic detectability of optoacoustic signals from low-concentration PEG-coated gold nanorods. International Journal of Nanomedicine, 2012, 7, 4373.	3.3	20
68	Harmonic Ultrasound Imaging of Nanosized Contrast Agents for Multimodal Molecular Diagnoses. IEEE Transactions on Instrumentation and Measurement, 2012, 61, 1848-1856.	2.4	41
69	Low-frequency ultrasound contrast enhancement behavior of a new nano-system for dual-mode imaging. , 2011, , .		Ο
70	A novel dual-frequency method for selective ultrasound imaging of targeted nanoparticles. , 2011, , .		4
71	Nanocomposites for multimodal molecular imaging. , 2011, , .		4
72	Hepatic Vessel Segmentation for 3D Planning of Liver Surgery. Academic Radiology, 2011, 18, 461-470.	1.3	57

## FRANCESCO CONVERSANO

#	Article	IF	CITATIONS
73	A quantitative and automatic echographic method for real-time localization of endovascular devices. IEEE Transactions on Ultrasonics, Ferroelectrics, and Frequency Control, 2011, 58, 2107-2117.	1.7	29
74	Advanced spectral analysis for automatic echographic monitoring of an evolving tumour mass. , 2011, , .		1
75	Magnetic/Silica Nanocomposites as Dualâ€Mode Contrast Agents for Combined Magnetic Resonance Imaging and Ultrasonography. Advanced Functional Materials, 2011, 21, 2548-2555.	7.8	82
76	Ultrasound detection of nanoparticle contrast agents for multimodal molecular imaging. , 2011, , .		2
77	Experimental assessment of gold nanorods for optoacoustic imaging in a tissue-mimicking phantom. , 2011, , .		1
78	Improving automatic segmentation of tissue-targeted nanoparticles on echographic images. , 2011, , .		9
79	Characterization of iron oxide-gold core-shell multifunctional nanoparticles in biomedical imaging. , 2011, , .		Ο
80	Optimal Enhancement Configuration of Silica Nanoparticles for Ultrasound Imaging and Automatic Detection at Conventional Diagnostic Frequencies. Investigative Radiology, 2010, 45, 715-724.	3.5	82
81	A new automatic phase mask filter for high-resolution brain venography at 3 T: theoretical background and experimental validation. Magnetic Resonance Imaging, 2010, 28, 511-519.	1.0	11
82	Full experimental modelling of a liver tissue mimicking phantom for medical ultrasound studies employing different hydrogels. Journal of Materials Science: Materials in Medicine, 2009, 20, 983-989.	1.7	32
83	Experimental investigation and theoretical modelling of the nonlinear acoustical behaviour of a liver tissue and comparison with a tissue mimicking hydrogel. Journal of Materials Science: Materials in Medicine, 2008, 19, 899-906.	1.7	19
84	Hydrogel based tissue mimicking phantom for <i>inâ€vitro</i> ultrasound contrast agents studies. Journal of Biomedical Materials Research - Part B Applied Biomaterials, 2008, 87B, 338-345.	1.6	42
85	Experimental Investigations of Nonlinearities and Destruction Mechanisms of an Experimental Phospholipid-Based Ultrasound Contrast Agent. Investigative Radiology, 2007, 42, 95-104.	3.5	29
86	Polymeric meshes for internal sutures with differentiated adhesion on the two sides. Journal of Materials Science: Materials in Medicine, 2005, 16, 289-296.	1.7	10
87	Low microbubble concentrations signal enhancement varying echograph electrical power. , 2005, , .		0
88	Cellulose Derivativeâ^'Hyaluronic Acid-Based Microporous Hydrogels Cross-Linked through Divinyl Sulfone (DVS) To Modulate Equilibrium Sorption Capacity and Network Stability. Biomacromolecules, 2004, 5, 92-96.	2.6	106
89	Ultrasound harmonic behaviour of artificial tissues. , 0, , .		1